Supplement of Atmos. Meas. Tech., 12, 4439–4453, 2019
https://doi.org/10.5194/amt-12-4439-2019-supplement

Atmospheric Measurement Techniques
Open Access
EGU

Supplement of

An IBBCEAS system for atmospheric measurements of glyoxal and methylglyoxal in the presence of high NO_2 concentrations

Jingwei Liu et al.

Correspondence to: Xin Li (li_xin@pku.edu.cn)

Supplement summary

Supplement pages: 10

Supplement sections: 1

Supplement tables: 1

Supplement figures: 7

Sections:

Tables:

Figures:

Section S1. Model simulation of evaluating the NO_2 photolytic convertor

In order to evaluate the NO_2 photolytic convertor (NPC) while sampling an atmospheric background of VOCs, a model simulation of the gas in photolytic cell was performed. Given the size of the photolysis cell (i.e., a cylinder with 60 mm length and 13.4 mm inner diameter) and the sampling flow rate of 2 L/min, the residence time of the sampled air in the cell is about 0.25 s. In such a short period, the productions of GLY and MGLY in the cell is negligible which can be verified by model simulations.

The model includes the full MCM chemistry (version 3.3.1, http://mcm.leeds.ac.uk/MCM/) for all NMHCs and their oxidation products. The initial concentrations of OH, HO_2, O_3, NO, HONO, CO, CH_4, C_2-C_{12} NMHCs are set to the average values

obtained during a field observation campaign in 2018 in Yangtze River Delta, China (see Table S1). The total OH reactivity due to NMHCs is 3.1 s^{-1}. The relative humidity, temperature, and pressure are constrained by the campaign averages, i.e., 60%, 300 K, 1007.65 hPa, respectively. The photolysis frequencies are constrained by values calculated from the spectral actinic flux inside the cell (Fig. S1). The spectral actinic flux is estimated by the LED emission spectrum and by the concentration change of NO, NO_2, and O_3 when NO_2 standard (100 ppb) is running through the system. The initial values of NO_2, GLY, MGLY are set to 60 ppb, 100 ppt, and 100 ppt, respectively. Figure S2 shows the calculated concentrations of NO_2, O_3, GLY, and MGLY for the period of 0.25 s residence time. While the NO_2 concentration drops from 60 ppb to 15 ppb leading to an increase of O_3 concentration by approximately 45 ppb, the change of GLY and MGLY concentrations is only around 1%. As shown in figure S3, the production rate of GLY and MGLY increases to around 5 ppb h^{-1} which could only result in maximumly 0.34 ppt increase of GLY and MGLY. Even if we increase the initial NMHCs concentration in the model by a factor of 10 (i.e., the OH reactivity due to NMHCs increases to 31 s^{-1}), the maximum production of GLY and MGLY within 250 ms is less than 2 ppt which is only 2% of their initial concentration (Fig. S4). Since the NMHCs concentration in the model represents typical atmospheric condition influenced by urban air pollution, our model simulation clearly shows that the NPC can be used in the field observations for removing NO_2 without additional production of GLY and MGLY.

Table S1. Initial concentration of species included in the model simulation.

Species	Concentration	Species	Concentration
OH	10^7 cm^{-3}	NO	0.60 ppb
HO2	10^9 cm^{-3}	HONO	0.45 ppb
CH4	1.9 ppm	CO	0.33 ppm
O3	70.00 ppb	SO2	1.33 ppb
NO2	60 ppb	MGLY	100.0 ppt
GLY	100.0 ppt	TOLUENE	0.515 ppb
C2H2	1.000 ppb	NC8H18	0.034 ppb
CBUT2ENE	0.050 ppb	EBENZ	0.140 ppb
C2H4	0.900 ppb	MXYL	0.045 ppb
C2H6	2.130 ppb	NC9H20	0.019 ppb
IC4H10	0.380 ppb	OXYL	0.076 ppb
IC5H12	0.330 ppb	STYRENE	0.017 ppb
NC4H10	0.650 ppb	IPBENZ	0.012 ppb
NC5H12	0.240 ppb	PBENZ	0.014 ppb
PENT1ENE	0.004 ppb	METHTOL	0.016 ppb
TPENT2ENE	0.002 ppb	PETHTOL	0.015 ppb
C5H8	0.233 ppb	NC10H22	0.017 ppb
CPENT2ENE	0.003 ppb	TM135B	0.014 ppb
M22C4	0.019 ppb	OETHTOL	0.036 ppb
M23C4	0.020 ppb	TM123B	0.014 ppb
M2PE	0.100 ppb	PXYL	0.045 ppb
M3PE	0.076 ppb	NC11H24	0.019 ppb
HEX1ENE	0.009 ppb	C3H8	2.010 ppb
NC6H14	0.130 ppb	C3H6	0.120 ppb
M2HEX	0.030 ppb	C4H6	0.005 ppb
CHEX	0.044 ppb	TM124B	0.016 ppb
M3HEX	0.041 ppb	TBUT2ENE	0.002 ppb
BENZENE	0.364 ppb	BUT1ENE	0.040 ppb
NC7H16	0.055 ppb		

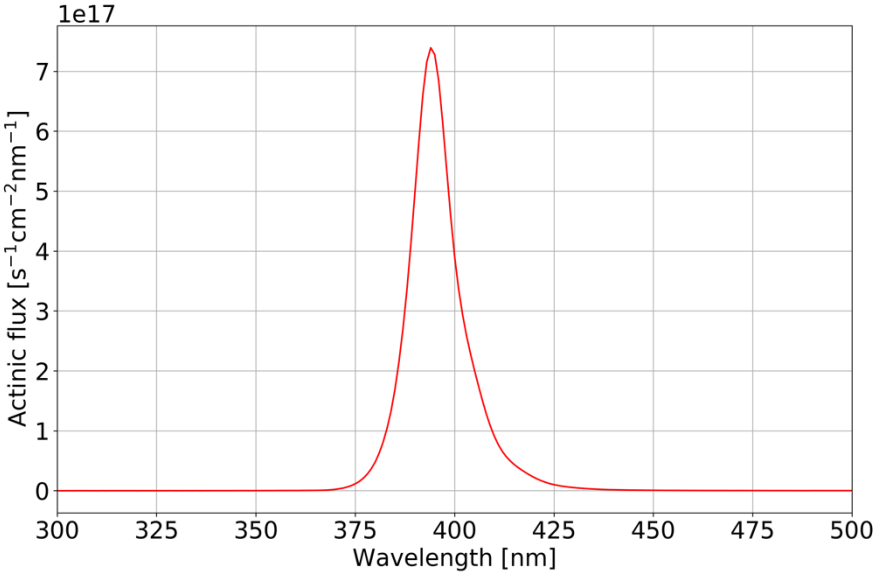

Figure S1. Spectral actinic flux inside the photolysis cell of the NO_2 photolytic convertor (NPC).

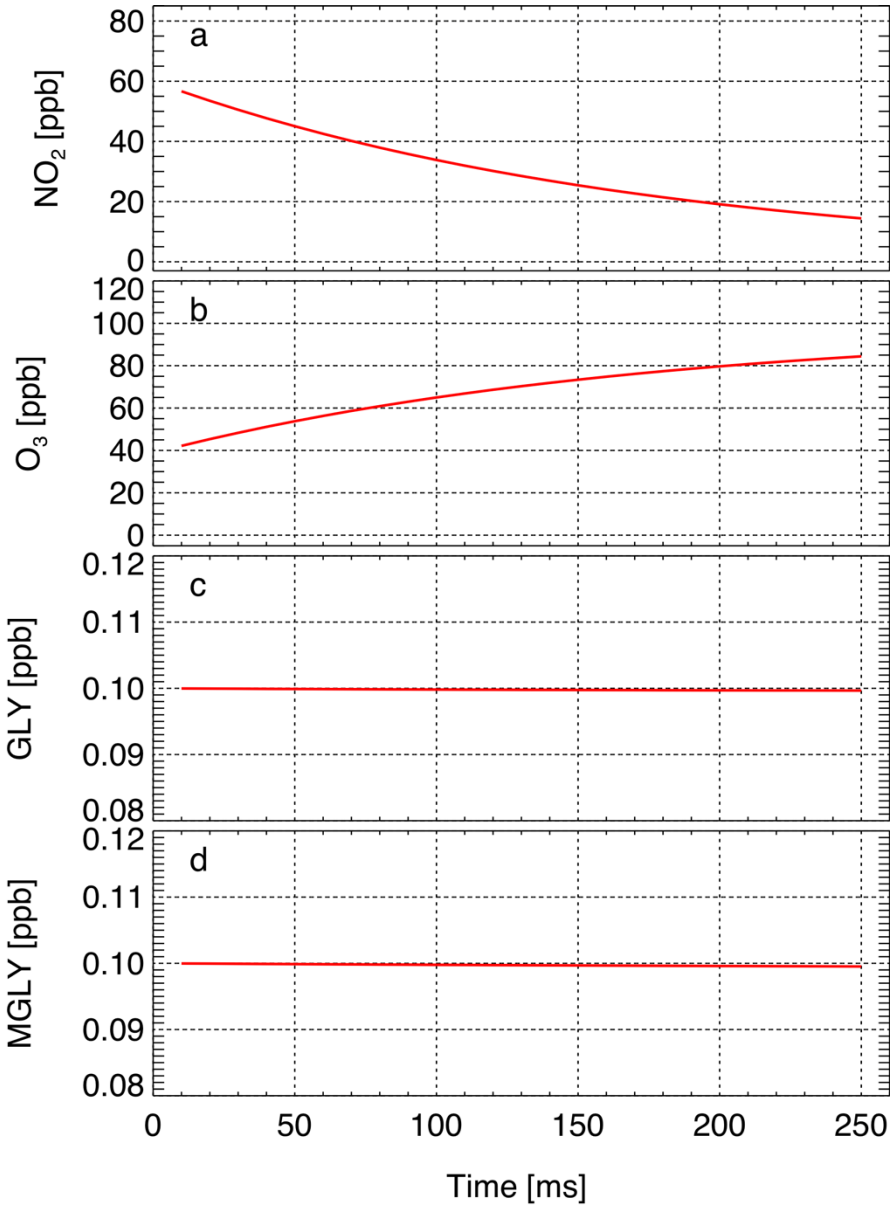

Figure S2. Model calculated concentrations of NO_2 (a), O_3 (b), GLY (c), and MGLY (d) in the photolysis cell of the NO_2 photolytic convertor. Note that the concentrations at 250 ms represent the condition of the sampled air exits the cell, since the residence time in the cell is about 250 ms.

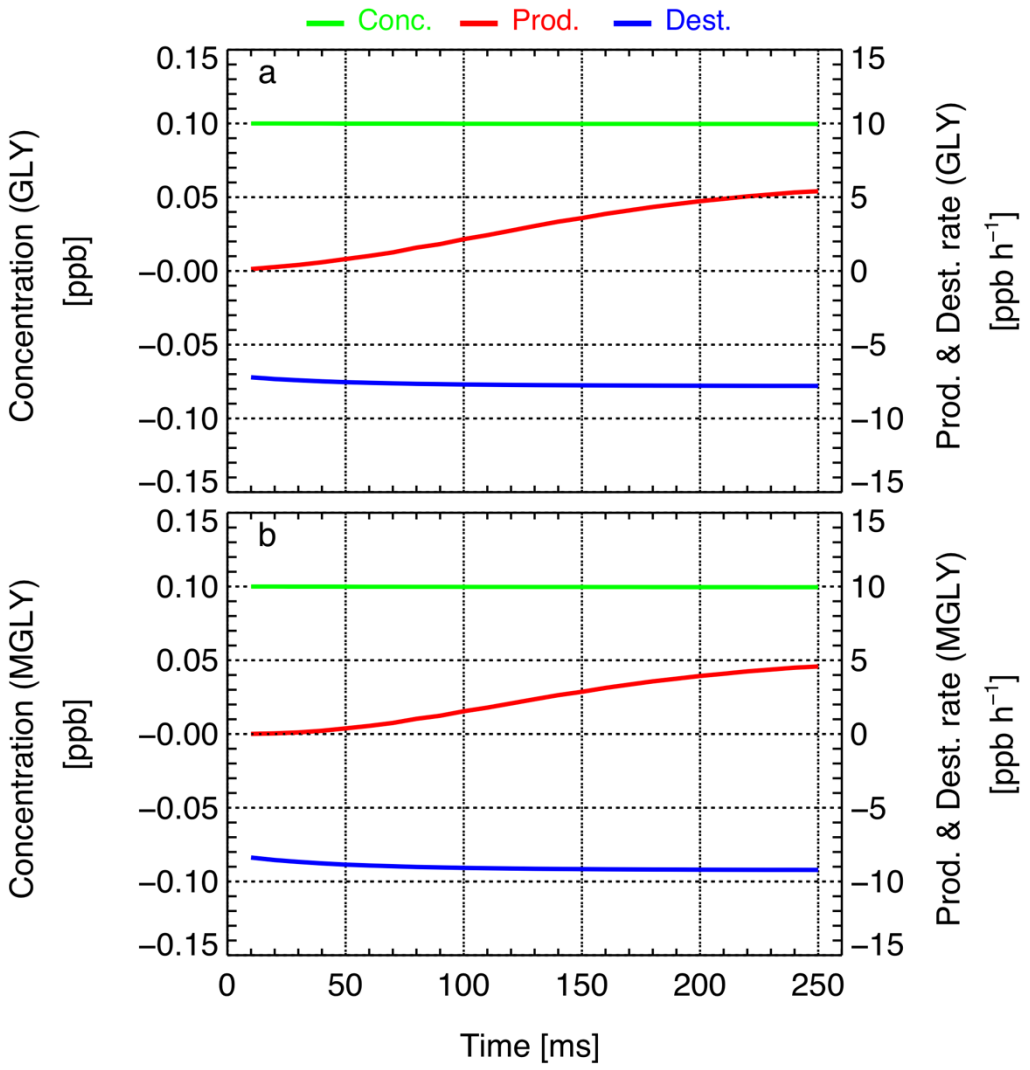

Figure S3. Model calculated concentrations (green), production rates (red), and destruction rates (blue) of GLY (a) and MGLY (b) in the photolysis cell of the NO_2 photolytic convertor. Note that the concentrations at 250 ms represent the condition of the sampled air exits the cell, since the residence time in the cell is about 250 ms.

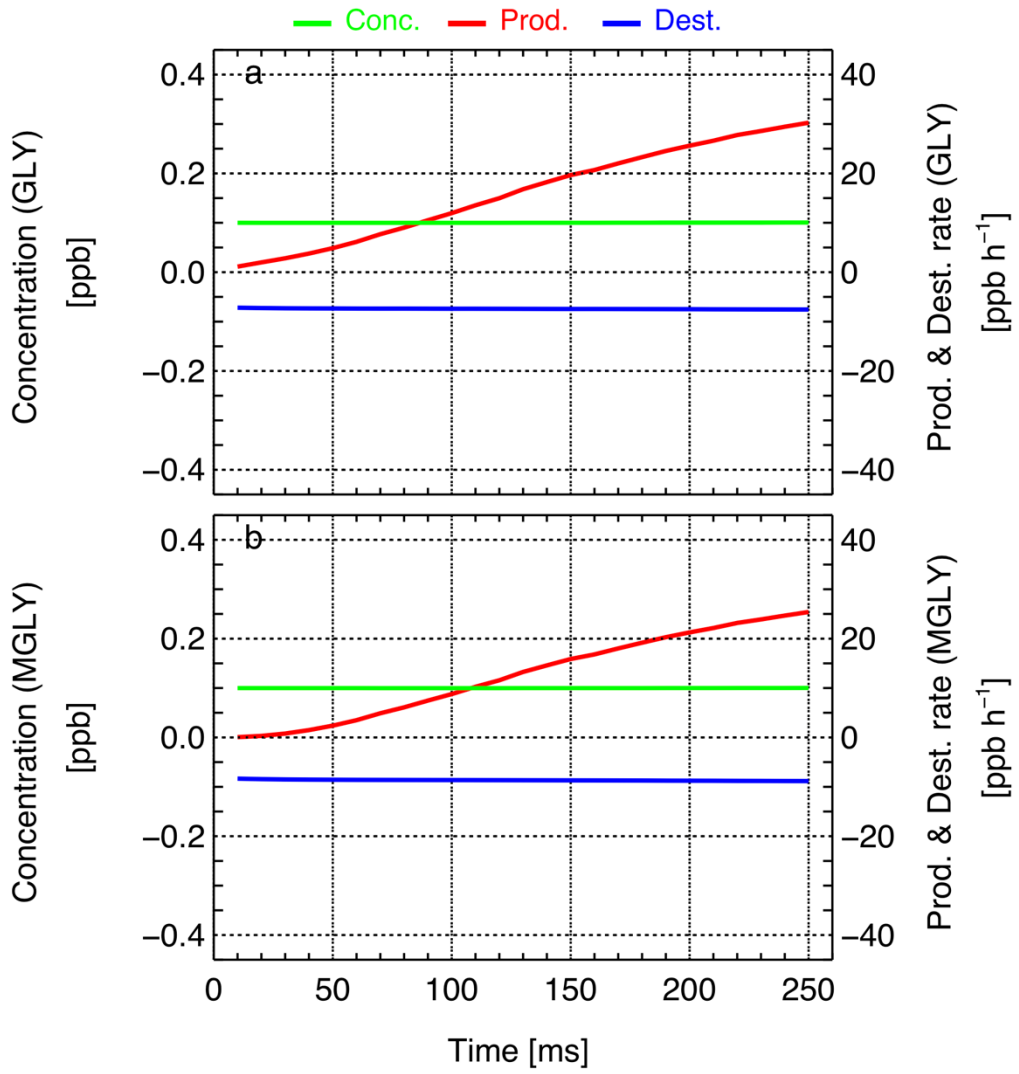

Figure S4. Model calculated concentration (green), production rate (red), and destruction rate (blue) of GLY (a) and MGLY (b) in the photolysis cell of the NO_2 converter. The initial concentrations of NMHCs in the model are set to 10 times of the values listed in in Table S1. Note that the concentrations at 250 ms represent the condition of the sampled air exits the cell, since the residence time in the cell is about 250 ms.

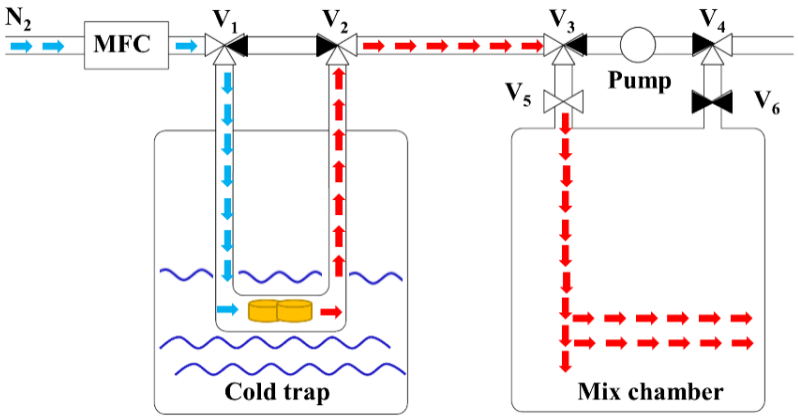

Figure S5. Diagram of the standard gas generator for GLY and MGLY. The temperature of cold trap (-72 ℃) is achieved by mixing dry ice and ethanol. The volume of the mixing chamber is 50 L. When mixing gases in the mix chamber, flow rate of the pump is set to 20 L/min.

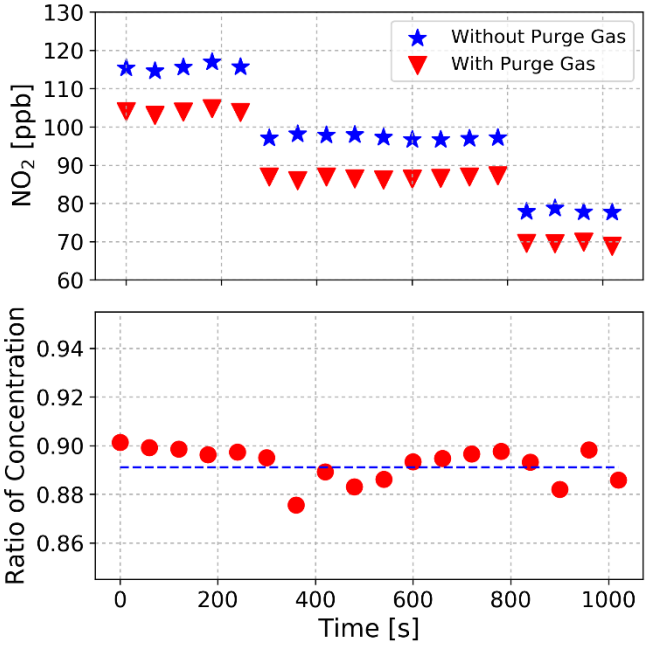

Figure S6. NO_2 concentrations measured with and without purge gas. The ratio of NO_2 concentration with 100 mL/min purge flows and 2 L/min sampling flow fluctuated around 0.89 (blue dotted line) and standard deviation of these ratios is 0.0056.

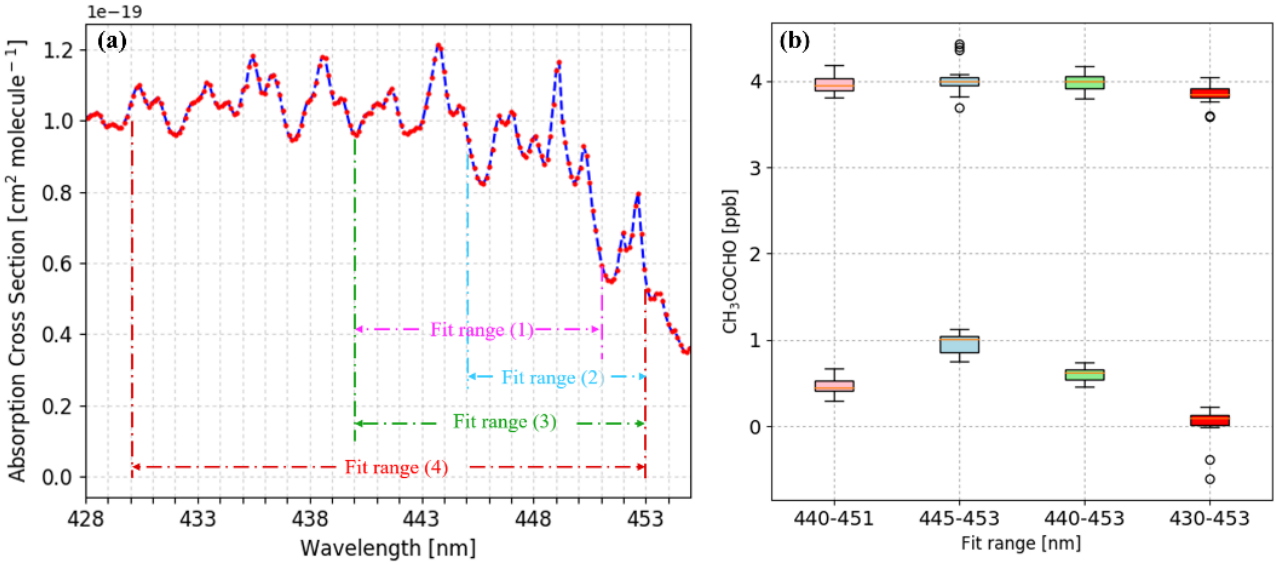

Figure S7. (a) Four spectral fit ranges (440-451 nm, 445-453 nm, 440-453 nm, and 430-453 nm) for MGLY. **(b)** Each spectral fit range was used to fit two experimental sets of MGLY produced by the standard gas generator. Experimental results of both sets indicated that fit range has a great influence on the fitted concentrations of MGLY.